AFSSAAE

Advances in Food Science, Sustainable Agriculture and Agroindustrial Engineering 2023, 6(3), 253-266
ISSN 2622-5921

ORIGINAL RESEARCH Open Access

In silico study of *Impatiens balsamina L.* for the screening of bioactive compounds as novel matrix metalloproteinase-1 inhibitor against photoaging

Sindi Fujiyanti and Mochamad Nurcholis*

Department of Food Science and Biotechnology, Faculty of Agricultural Technology, Universitas Brawijaya, Malang, Indonesia

KEYWORDS

In silico

Impatiens balsamina L.

Matrix metalloproteinase-1

Photoaging

ABSTRACT

Photoaging is skin aging caused by exposure to UV rays, which increases the expression of matrix metalloproteinase-1 (MMP-1). The photoaging process is related to the degradation of collagen types I and III in the extracellular matrix by MMP-1, which causes wrinkles on the skin. MMP-1 inhibitors from natural products have the potency as anti-photoaging. This study aims to screen the potency of bioactive compounds from *Impatiens balsamina L*. as MMP-1 inhibitors through in silico studies. The best test ligands were selected based on bioavailability, pharmacokinetics, toxicity, and molecular docking tests against the target protein MMP-1 (PDB ID: 1HFC) compared to that of control ligands (PLH and doxycycline). Peonidin, kaempferol, and pelargonidin were selected as the best test ligands because they accomplish the characteristics of bioavailability, pharmacokinetics, and toxicity. Based on molecular docking results, those test ligands have better binding affinity than that of control ligands, as indicated by rerank scores of -108.807 kcal/mol, -99.9796 kcal/mol, and -98.9128 kcal/mol, respectively. Those test ligands also formed the same interactions with control ligands at residues Ala182, Asn180, Glu219, and Leu181. The results suggest peonidin, kaempferol, and pelargonidin were candidates for anti-photoaging agents through MMP-1 inhibition.

Introduction

UV exposure is the main external factor that causes photoaging, which is characterized by the formation of wrinkles on the skin. Wrinkles can form due to collagen degradation, causing damage to the extracellular matrix (Pittayapruek et al., 2016). The extracellular matrix is the main component of the dermis skin layer that occupies the intercellular space and plays a role in facilitating intercellular communication (Sparavigna, 2020). The major components of the extracellular matrix are collagen types I and III, which comprise more than 80% and 15% of the total collagen, respectively (Reilly and Lozano, 2021). The main collagenolytic enzyme that plays a role in the degradation of collagen types I and III in the extracellular matrix is matrix metalloproteinase-1 (MMP-1). UV exposure increases the expression of MMP-1, which leads to photoaging due to the increased activity of MMP-1 in degrading collagen types I and III in the extracellular matrix (Yasmeen and Gupta, 2019). Therefore, anti-photoaging agents are needed to inhibit the activity of MMP-1 in degrading collagen types I and III.

In recent years, using natural ingredients with the potency for anti-photoaging in skin care products has been gaining more attention and is expected to continue growing (Amer et al., 2021). *Impatiens balsamina L.*, commonly known as "Pacar Air" in Indonesia, is one of the plants with the potency as an anti-photoaging agent through inhibition of MMP-1 activity. *I. balsamina L.* contains various bioactive compounds (i.e., phenolic compounds, quinones, and triterpenoids) (Szewczyk, 2018). In vitro studies have shown that phenolic compounds such as apigenin, kaempferol, chrysin, quercetin, luteolin, and myricetin are known to exhibit inhibitory activity against MMP-1 (Ronsisvalle et al., 2020). *I. balsamina L.* can be found in several regions in Indonesia as a wild or ornamental plant. *I. balsamina L.* is easy to plant and grows well in humid places (Utami, 2014). Currently, the utilization of *I. balsamina L.* is still

*Corresponding author
E-mail address: cholis_federer@ub.ac.id

Received on 13 May 2023, Revised on 18 September 2023, Accepted on 20 September 2023

limited for religious activities. Therefore, exploring the utilization of *I. balsamina L.* and its potential activity as MMP-1 inhibitor for anti-photoaging is necessary.

In silico is a research method performed via computer simulation, thus reducing the need for animal models and decreasing the time and cost of studies (Brogi et al., 2020). In silico methods have been widely used to predict the potency of bioactive compounds through several parameters (such as prediction of bioavailability, pharmacokinetics, toxicity, and molecular docking) to obtain potential and non-toxic compounds (Shaker et al., 2021). Therefore, this study aimed to predict the potential of bioactive compounds of *I. balsamina L.* as anti-photoaging candidates through MMP-1 inhibition using in silico methods.

Research Methods

Materials

This study used the 3D structure of MMP-1 (PDB ID: 1HFC) as the target protein, 3D structures, and canonical SMILES of test ligands (50 bioactive compounds of *I. balsamina L.* obtained through literature studies) and control ligands (methylamino-phenylalanyl-leucyl-hydroxamic acid (PLH) and doxycycline). PLH is a natural inhibitor of MMP-1, and doxycycline is the only MMP inhibitor approved by the Food and Drug Administration (FDA). This study also used a laptop with Intel ® Celeron ® N4000 CPU @ 1.10GHz 1.10 GHz processor, 4 GB RAM, 64-bit Windows 10 Home Single Language operating system, and some software including Molegro Virtual Docker, and web-based applications including PubChem, SwissADME, pkCSM, and ProTox-II.

Methods

Collecting ligands and target protein

The 3D structures and canonical SMILES of the test and control ligands were downloaded from the PubChem database (https://pubchem.ncbi.nlm.nih.gov/). The 3D structures of ligands were saved in SDF format. In addition, the 3D structure of the target protein (MMP-1) was downloaded from the Protein Data Bank database (https://www.rcsb.org/) with PDB ID 1HFC and saved in PDB format.

Bioavailability prediction

Bioavailability prediction was performed by entering the canonical SMILES of the test and control ligands on SwissADME (http://www.swissadme.ch/). The parameters evaluated in bioavailability prediction are Lipinski's rule parameters, including molecular weight, number of hydrogen bond acceptors, number of hydrogen bond donors, and lipophilicity.

Pharmacokinetic prediction

Pharmacokinetic prediction was performed by entering canonical SMILES of test and control ligands on pkCSM (https://biosig.lab.uq.edu.au/pkcsm/prediction). Parameters evaluated in pharmacokinetic prediction include intestinal absorption, skin permeability, VDss (The steady-state volume of distribution), CYP3A4 inhibitor, CYP2D6 inhibitor, and total clearance.

Toxicity prediction

Toxicity prediction was performed by entering the canonical SMILES of test and control ligands on ProTox-II (https://tox-new.charite.de/protox_II/) and pkCSM. ProTox-II was used to evaluate the parameters of hepatotoxicity, carcinogenicity, immunotoxicity, cytotoxicity, and lethal dose 50 (LD_{50}). While pkCSM was used to evaluate the parameters of AMES toxicity (mutagenicity), maximum tolerated dose (highest dose of the compound without producing toxicity in the body), and skin sensitization.

Validation of molecular docking method

Validation was carried out by redocking the reference ligand (PLH) to the prepared target protein using Molegro Virtual Docker. The target protein was prepared by removing its natural ligand and water molecules. Validation is evaluated based on the root-mean-square deviation (RMSD) value ≤ 2 Å that indicates the redocking parameters are acceptable and can be used in the molecular docking process between the test ligand and the target protein.

Molecular docking

Molecular docking was performed on the test ligands that accomplish bioavailability, pharmacokinetics, and toxicity parameters. All processes in molecular docking were performed using Molegro Virtual Docker. Molecular docking was performed by docking the test and control ligands to target protein and then visualizing the molecular docking results. Parameters evaluated in molecular docking include rerank score and the interaction between the test ligand and target protein.

Results and Discussion

Bioavailability prediction

Bioavailability prediction was carried out to determine the potential absorption of bioactive compounds from *I. balsamina L.* in the body based on physicochemical properties of the compounds evaluated using Lipinski's rule (Lipinski et al., 2012). Based on Lipinski's rule, a bioactive compound should not have more than one violation of the parameters proposed in the rule, which are: molecular weight no more than 500 g/mol, the number of hydrogen bond donors no more than 5, the number of hydrogen bond acceptors no more than 10, and lipophilicity (log P) no more than 5 (Lipinski et al., 2012). Lipinski's rule states that any compound which violates more than one of these parameters is more likely to have poor absorption (Lipinski et al., 2012). The absorption rate of the compounds depends on the permeability through the cell membrane (Kalepu et al., 2013). The absorption process of compounds both orally (Arivazhahan, 2019) and non-orally (Ruela et al., 2016) through the skin is known to pass through the phospholipid bilayer of the cell membrane, which has a hydrophilic head and lipophilic tail. The bioavailability prediction results are shown in Table 1, and the percentage of bioactive compounds that accomplish Lipinski's rule parameters are shown in Figure 1.

Molecular weight is one of the parameters that can affect the absorption process of bioactive compounds in the body. Based on the prediction results, 46 test ligands (92%) have molecular weight less than 500 g/mol. Bioactive compounds with a molecular weight of not more than 500 g/mol can easily pass through the phospholipid bilayer and have good absorption potential (Ruswanto et al., 2022). Another parameter is the number of hydrogen bond donors and acceptors related to hydrogen bonding capacity. Based on the prediction results, 39 test ligands (78%) have no more than 5 hydrogen bond donors, and 43 test ligands (86%) have no more than 10 hydrogen bond acceptors. Compounds that can form hydrogen bonds can increase the potential for absorption and interaction with their biomolecular targets. However, too high hydrogen bonding capacity may reduce the permeability of a compound to pass through the phospholipid bilayer because it can interact and form hydrogen bonds, such as with water, causing the compounds to have difficulty passing through the lipophilic region (Coimbra et al., 2021). Lipophilicity is a parameter that shows the ratio of solubility of compounds in organic solvents (octanol) and water determined from the logarithm of the partition coefficient (log P) (Lipinski et al., 2012). Based on the prediction results, 36 test ligands (72%) have a log P value of less than 5. Compounds with high lipophilicity (log P > 5) tend to have poor solubility in the aqueous phase and can be retained longer in the phospholipid bilayer. In addition, compounds with low lipophilicity (a negative log P) indicate that the molecule is hydrophilic, which makes it more difficult to pass through the phospholipid bilayer (Ruswanto et al., 2022). Thus, the process of passing through the phospholipid bilayer is disrupted, causing the bioactive compounds to be poorly absorbed and have low bioavailability. Therefore, a compound is not expected to have lipophilicity properties that are too high (log P > 5) or too low (a negative log P).

The bioavailability prediction results show that most of the bioactive compounds of *I. balsamina. L* are predicted to have good bioavailability. A total of 41 test ligands are known to accomplish 3 to 4 parameters of Lipinski's rule as expected. These test ligands also showed better bioavailability potential than the control ligand doxycycline, which violated two parameters of Lipinski's rule.

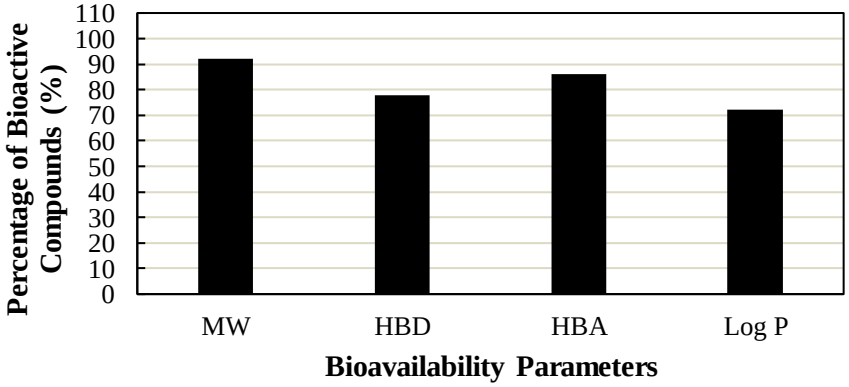

Figure 1. Percentage of bioactive compounds from *I. balsamina L*. based on bioavailability parameters. MW = Molecular weight; HBD = Hydrogen Bond Donor; HBA = Hydrogen Bond Acceptor; and Log P = Lipophilicity.

Table 1. Bioavailability prediction results

Bioactive Compounds	Molecular Weight (g/mol)	Hydrogen Bond Donor	Hydrogen Bond Acceptor	Lipophilicity (log P)
PLH*	349.42	4	4	1.32
Doxycycline*	444.43	6	9	-0.28
Kaempferol	286.24	4	6	1.58
Astragalin	448.38	7	11	-0.25
Nicotiflorin	594.52	9	15	-0.73
Asiaticalin	448.38	7	11	-0.25
Quercetin	302.24	5	7	1.23
Isoquercitrin	464.38	8	12	-0.25
Rutin	610.52	10	16	-1.29
Dihydromyricetin	320.25	6	8	0.22
Myricetin	318.24	6	8	0.79
Cyanidin	287.24	5	6	0.32
Cyanidin 3-O-glucoside	484.84	8	11	-1.99
Delphinidin	338.70	6	7	-0.98
Malvidin	331.30	4	7	0.92
Pelargonidin	271.24	4	5	0.93
Pelargonidin 3-glucoside	433.39	7	10	-0.73
Pelargonin chloride	630.98	10	15	-3.91
Peonidin	301.27	4	6	0.97
Gallic acid	170.12	4	5	0.21
Gentisic acid	154.12	3	4	0.74
p-hydroxybenzoic acid	138.12	2	3	1.05
Protocatechuic acid	154.12	3	4	0.65
Salicylic acid	138.12	2	3	1.24
Syringic acid	198.17	2	5	0.99
Vanillic acid	168.15	2	4	1.08
Caffeic acid	180.16	3	4	0.93
Cinnamic acid	148.16	1	2	1.79
3-hydroxycinnamic acids	164.16	2	3	1.36
Ferulic acid	194.18	2	4	1.36
cis-ferulic acid	194,18	2	4	1.36
p-coumaric acid	164.16	2	3	1.26
cis-p-coumaric acid	164.16	2	3	1.26
Sinapic acid	224.21	2	5	1.31
cis-sinapic acid	224.21	2	5	1.31
Coumarin	146.14	0	2	1.82
Scopoletin	192.17	1	4	1.52
Fraxidin	222.19	1	5	1.49
2-Methoxy-1,4-naphthoquinone	188.18	0	3	1.43
Lawsone	174.15	1	3	0.96
Impatienolate	418.31	0	6	-3.14
Balsaminolate	240.19	1	4	-1.72
Balsaminone A	344.32	1	5	3.40
Balsaminone B	506.46	4	10	1.60
Hydroquinone	110.11	2	2	0.87
Anthraquinone	208.21	0	2	2.64
alpha-Spinasterol	412.69	1	1	6.87
Hexahydrofarnesyl acetone	268.48	0	1	5.66
Lauric acid	200.32	1	2	3.51
Myristic acid	228.37	1	2	4.45
beta-Ionone	192.30	0	1	3.22
Phytol	296.53	1	1	6.22

Note: * = Control ligands; Red color indicates values that do not meet the parameters of Lipinski's rule.

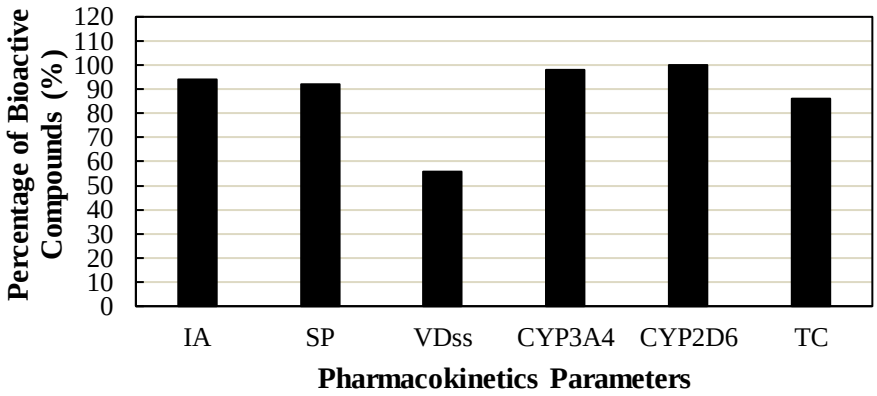

Figure 2. Percentage of bioactive compounds from *I. balsamina L.* based on pharmacokinetic parameters. IA = Intestinal Absorption; SP = Skin Permeability; VDss = Volume of Distribution; CYP3A4 = CYP3A4 Inhibitor; CYP2D6 = CYP2D6 Inhibitor; and TC = Total Clearance.

Pharmacokinetic prediction

Pharmacokinetic prediction was carried out to predict the movement of bioactive compounds from *I. balsamina L.* throughout the body, including the absorption, distribution, metabolism, and excretion (ADME) process (Roy et al., 2015). Based on pharmacokinetic predictions, a compound is known to have good pharmacokinetic properties if it accomplishes the ADME profile which includes an intestinal absorption value of more than 30%, skin permeability (log Kp) less than -2.5 cm/hour, VDss more than -0.15 log L/kg, not an inhibitor of CYP2D6 and CYP3A4, and a high total clearance (Firdausy et al., 2020). The pharmacokinetic prediction results are shown in Table 2 and the percentage of bioactive compounds that accomplish pharmacokinetic parameters are shown in Figure 2.

The absorption of a compound is one of the parameters to determine the bioactive compound's potential to be absorbed into the body. The absorption of compounds is predicted based on intestinal absorption and skin permeability parameters. Based on the prediction results, 47 test ligands (94%) accomplish the intestinal absorption parameters, and 46 test ligands (92%) accomplish the skin permeability parameters. A bioactive compound that is administered orally needs to go through the absorption process of the intestinal tract, which is the main place of oral absorption before it is distributed and reached the desired target and shows its therapeutic effect (Azman et al., 2022). In addition, absorption is also predicted based on skin permeability parameters to predict the absorption potential of bioactive compounds administered through the skin.

Distribution is a parameter that predicts the passage of a drug compound through the bloodstream to body tissues. The distribution process can affect the amount of drug compound that can reach the target (Paul, 2019). The volume of distribution (VDss) is one of the important parameters in pharmacokinetic parameters. The VDss is a parameter that predicts the tendency of drug compounds to be in blood plasma or distributed to extravascular compartments (outside blood vessels) such as interstitial and intracellular spaces. Based on the prediction results, 28 test ligands (56%) accomplish the VDss parameter. Bioactive compounds with high log VDss values indicate higher compound distribution in extravascular compartments than in blood plasma (intravascular) (Chatterjee, et al., 2021). The target protein (MMP-1) can cause the degradation of extracellular matrix (ECM) components that occupy the intercellular space in the extravascular compartment (Sparavigna, 2020). Based on this, a compound with a high log VDss value (> -0.15) is needed so that the distribution of the compound is higher toward the extravascular compartment (Chatterjee, et al., 2021).

Metabolism is a parameter related to the chemical change process of compounds to become more hydrophilic to facilitate the removal of compounds from the body catalyzed by enzymes. Enzymes that play a role in the metabolism of compounds are cytochrome P-450 (CYP), which catalyzes the oxidation of many drug compounds that enter the body (Mcginnity and Grime, 2017). The two most abundant CYP enzymes are CYP3A4 and CYP2D6, which metabolize about 50% and 30% of compounds. Inhibition of CYP3A4 and CYP2D6 may interfere with the metabolic process, causing therapeutic effects not to be achieved and leading to an increased risk of unexpected side effects and toxicity (Feltrin et al., 2020). Therefore, it is necessary to evaluate that the drug compound is not an inhibitor of CYP3A4 and CYP2D6. Based on the prediction results, most of the test ligands showed that they were not CYP3A4 (99%) and CYP2D6 (100%) inhibitors, and only one compound, Balsaminone A, showed results as a CYP3A4 inhibitor.

Table 2. Pharmacokinetic prediction results

Bioactive Compounds	IA	SP	VDss	CYP3A4	CYP2D6	TC
PLH*	55,14	-2.97	-0.54	No	No	0.55
Doxycycline*	44,52	-2.74	1.14	No	No	0.22
Kaempferol	74,29	-2.74	1.27	No	No	0.48
Astragalin	48,05	-2.74	1.44	No	No	0.46
Nicotiflorin	30,74	-2.74	1.71	No	No	-0.16
Asiaticalin	48,05	-2.74	1.44	No	No	0.46
Quercetin	77,21	-2.74	1.56	No	No	0.41
Isoquercitrin	48,00	-2.74	1.85	No	No	0.39
Rutin	23,45	-2.74	1.66	No	No	-0.37
Dihydromyricetin	58,92	-2.74	1.66	No	No	0.28
Myricetin	65,93	-2.74	1.32	No	No	0.42
Cyanidin	87,30	-2.74	0.95	No	No	0.53
Cyanidin 3-O-glucoside	29,93	-2.74	1.49	No	No	0.55
Delphinidin	61,92	-2.74	0.97	No	No	0.57
Malvidin	88,79	-2.74	0.76	No	No	0.69
Pelargonidin	87,29	-2.74	0.65	No	No	0.58
Pelargonidin 3-glucoside	48,35	-2.74	0.98	No	No	0.56
Pelargonin chloride	0	-2.74	0.87	No	No	0.14
Peonidin	89,16	-2.74	0.56	No	No	0.63
Gallic acid	43,37	-2.74	-1.86	No	No	0.52
Gentisic acid	80,08	-2.74	-1.52	No	No	0.59
p-hydroxybenzoic acid	83,96	-2.72	-1.56	No	No	0.59
Protocatechuic acid	71,17	-2.72	-1.30	No	No	0.55
Salicylic acid	83,89	-2.72	-1.57	No	No	0.61
Syringic acid	73,08	-2.74	-1.44	No	No	0.65
Vanillic acid	78,15	-2.73	-1.74	No	No	0.63
Caffeic acid	69,41	-2.72	-1.10	No	No	0.51
Cinnamic acid	94,83	-2.70	-1.05	No	No	0.78
3-hydroxycinnamic acids	92,86	-2.71	-1.16	No	No	0.66
Ferulic acid	93,69	-2.72	-1.37	No	No	0.62
cis-ferulic acid	93,69	-2.72	-1.37	No	No	0.62
p-coumaric acid	93,49	-2.72	-1.15	No	No	0.66
cis-p-coumaric acid	93,49	-2.72	-1.15	No	No	0.66
Sinapic acid	93,06	-2.73	-1.11	No	No	0.72
cis-sinapic acid	93,06	-2.73	-1.11	No	No	0.72
Coumarin	97,34	-1.92	-0.14	No	No	0.97
Scopoletin	95,28	-2.94	0.03	No	No	0.73
Fraxidin	95,18	-3.02	-0.06	No	No	0.72
2-Methoxy-1,4-naphthoquinone	97,42	-2.62	-0.06	No	No	0.22
Lawsone	93,85	-3.04	0.01	No	No	0.15
Impatienolate	54,90	-2.83	-0.34	No	No	1.63
Balsaminolate	78,51	-3.69	-0.20	No	No	0.89
Balsaminone A	95,63	-2.74	-0.77	Yes	No	0.18
Balsaminone B	67,41	-2.74	-0.97	No	No	0.12
Hydroquinone	86,86	-2.62	-0.02	No	No	0.52
Anthraquinone	99,06	-2.12	0.23	No	No	0.18
alpha-Spinasterol	94,97	-2.78	0.18	No	No	0.61
Hexahydrofarnesyl acetone	93,66	-2.33	0.50	No	No	1.52
Lauric acid	93,38	-2.69	-0.63	No	No	1.62
Myristic acid	92,69	-2.71	-0.58	No	No	1.69
beta-Ionone	95,44	-1.67	0.32	No	No	1.32
Phytol	90,71	-2.58	0.47	No	No	1.69

Note: * = Control ligands; IA = Intestinal Absorption (%); SP = Skin Permeability (cm/hour); VDss = Volume of Distribution (log L/kg); CYP3A4 = CYP3A4 inhibitor; CYP2D6 = CYP2D6 inhibitor; and TC = Total clearance; Red color indicates values that do not meet the parameters.

Excretion is the last stage in the ADME process that describes the processes of removing compounds from the body. It can be predicted based on the total excretion parameter (CLtot), which is the sum of all the removal processes from the body (Pires et al., 2015). The CLtot value is related to the half-life of the compound. The higher the CLtot value, the less time it takes to remove the compounds from the body (Bardal, et al., 2011). The control ligand (doxycycline) value is used as a reference to select the test ligands that have the potential to be well excreted. Based on the prediction results, 43 test ligands (86%) were found to have higher CLtot values than doxycycline.

Thus, the pharmacokinetic prediction results showed that most of the bioactive compounds from *I. balsamina L.* had good absorption, distribution, metabolism, and excretion (ADME) potential, with 19 test ligands accomplishing all the pharmacokinetic parameters.

Toxicity prediction

Toxicity prediction is carried out to predict the safety of a compound by evaluating the potentially harmful risks that can be caused to the body both orally and non-orally administered through the skin (Banerjee et al., 2018). Based on toxicity prediction, a compound is predicted to be non-toxic if it has a maximum tolerated dose (MTD) value of more than 0.477 log mg/kg/day (Pires et al., 2015), LD50 is more than 2000 mg/kg because it is considered to have low toxicity (Morris-Schaffer and McCoy, 2021), shows "No" results on AMES toxicity (mutagenicity) and skin sensitization (Pires et al., 2015), and show "Inactive" results on hepatotoxicity, carcinogenicity, immunotoxicity, and cytotoxicity parameters (Banerjee et al., 2018). The toxicity prediction results are shown in Table 3 and the percentage of bioactive compounds that accomplish toxicity parameters are shown in Figure 3.

Mutagenicity is a parameter used to identify the possibility of compounds that can cause genetic mutations. The prediction results show that 48 test ligands (96%) were not mutagenic. Maximum tolerated dose (MTD) is a parameter that estimates the highest dose of a compound without producing toxicity and causing unwanted side effects (Liu et al., 2016). The greater the tolerated dose level of the compounds, the greater the possibility of a high level of toxicity tolerance, which indicates that the bioactive compound is not too toxic (Ye et al., 2021). Based on the prediction results, 36 test ligands (72%) have high MTD values, which are predicted to be less toxic and tolerable by the body. Skin sensitization is a parameter to evaluate the safety of a compound administered non-orally through the skin by evaluating the possibility of the bioactive compound being allergenic and irritant or not (Pires et al., 2015). Based on the prediction results, 43 test ligands (86%) did not cause skin sensitization. Lethal dose 50 (LD50) is a parameter used to evaluate the potential acute toxicity of a compound. Based on the LD50 parameter, compounds with an LD50 of less than 50 mg/kg are highly toxic, while compounds with an LD50 of more than 2000 mg/kg are low toxic (Morris-Schaffer and McCoy, 2021). Therefore, based on the LD50 parameter, 29 test ligands (58%) are predicted to have low toxicity. Hepatotoxicity, carcinogenicity, immunotoxicity, and cytotoxicity are parameters used to evaluate the toxic properties of compounds that can cause impaired liver function, the onset of cancer in the body, harm the immune system, and cell damage or death (Banerjee et al., 2018). The findings confirmed that most of the test ligands are non-toxic to these parameters, indicated by the "inactive" results.

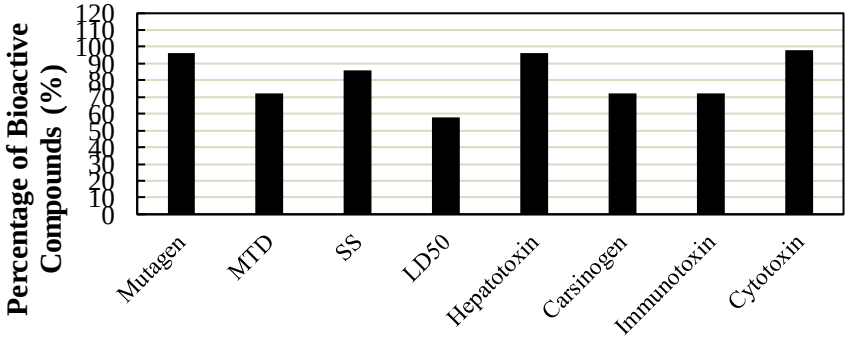

Figure 3. Percentage of bioactive compounds from *I. balsamina L.* based on toxicity parameters. Mutagen = Mutagenicity; MTD = Maximum Tolerated Dose; SS = Skin Sensitization; LD50 = Lethal Dose 50; Hepatotoxin = Hepatotoxicity; Carcinogen = Carcinogenicity; Immunotoxin = Immunotoxicity; and Cytotoxin = Cytotoxicity.

Table 3. Toxicity prediction results

Bioactive Compounds	M	MTD	SS	LD_{50}	HT	CG	IT	CT
PLH*	No	0.497	No	2287	Inactive	Inactive	Inactive	Inactive
Doxycycline*	No	0.294	No	2240	Active	Inactive	Active	Inactive
Kaempferol	No	0.531	No	3919	Inactive	Inactive	Inactive	Inactive
Astragalin	No	0.582	No	5000	Inactive	Inactive	Inactive	Inactive
Nicotiflorin	No	0.481	No	5000	Inactive	Inactive	Active	Inactive
Asiaticalin	No	0.582	No	5000	Inactive	Inactive	Inactive	Inactive
Quercetin	No	0.499	No	159	Inactive	Active	Inactive	Inactive
Isoquercitrin	No	0.569	No	5000	Inactive	Inactive	Active	Inactive
Rutin	No	0.452	No	5000	Inactive	Inactive	Active	Inactive
Dihydromyricetin	No	0.400	No	2000	Inactive	Active	Inactive	Inactive
Myricetin	No	0.510	No	159	Inactive	Active	Inactive	Inactive
Cyanidin	No	0.497	No	5000	Inactive	Active	Inactive	Inactive
Cyanidin 3-O-glucoside	No	0.562	No	5000	Inactive	Inactive	Active	Inactive
Delphinidin	No	0.503	No	5000	Inactive	Inactive	Inactive	Inactive
Malvidin	No	0.554	No	5000	Inactive	Inactive	Active	Inactive
Pelargonidin	No	0.501	No	3919	Inactive	Inactive	Inactive	Inactive
Pelargonidin 3-glucoside	No	0.526	No	5000	Inactive	Inactive	Inactive	Inactive
Pelargonin chloride	No	0.428	No	5000	Inactive	Inactive	Inactive	Inactive
Peonidin	No	0.568	No	5000	Inactive	Inactive	Inactive	Inactive
Gallic acid	No	0.700	No	2000	Inactive	Active	Inactive	Inactive
Gentisic acid	No	1.261	No	4500	Inactive	Inactive	Inactive	Inactive
p-hydroxybenzoic acid	No	0.846	No	2200	Inactive	Inactive	Inactive	Inactive
Protocatechuic acid	No	0.814	No	2000	Inactive	Active	Inactive	Inactive
Salicylic acid	No	0.610	No	1034	Active	Inactive	Inactive	Inactive
Syringic acid	No	1.374	No	1700	Inactive	Inactive	Inactive	Inactive
Vanillic acid	No	0.719	No	2000	Inactive	Inactive	Inactive	Inactive
Caffeic acid	No	1.145	No	2980	Inactive	Active	Inactive	Inactive
Cinnamic acid	No	1.110	No	2500	Active	Inactive	Inactive	Inactive
3-hydroxycinnamic acids	No	1.232	No	2980	Inactive	Active	Inactive	Inactive
Ferulic acid	No	1.082	No	1772	Inactive	Inactive	Active	Inactive
cis-ferulic acid	No	1.082	No	1772	Inactive	Inactive	Active	Inactive
p-coumaric acid	No	1.111	No	2850	Inactive	Active	Inactive	Inactive
cis-p-coumaric acid	No	1.111	No	2850	Inactive	Active	Inactive	Inactive
Sinapic acid	No	1.193	No	1772	Inactive	Inactive	Active	Inactive
cis-sinapic acid	No	1.193	No	1772	Inactive	Inactive	Active	Inactive
Coumarin	No	0.435	No	196	Inactive	Active	Inactive	Active
Scopoletin	No	0.614	No	3800	Inactive	Active	Active	Inactive
Fraxidin	No	0.647	No	3800	Inactive	Inactive	Active	Inactive
2-Methoxy-1,4-naphthoquinone	No	0.918	No	2000	Inactive	Inactive	Inactive	Inactive
Lawsone	No	0.976	No	8000	Inactive	Inactive	Inactive	Inactive
Impatienolate	No	-0.402	No	680	Inactive	Inactive	Inactive	Inactive
Balsaminolate	No	0.502	No	2000	Inactive	Inactive	Inactive	Inactive
Balsaminone A	Yes	0.339	No	450	Inactive	Active	Active	Inactive
Balsaminone B	No	0.447	No	5000	Inactive	Inactive	Active	Inactive
Hydroquinone	No	0.707	Yes	225	Inactive	Active	Inactive	Inactive
Anthraquinone	Yes	0.291	Yes	5000	Inactive	Inactive	Inactive	Inactive
alpha-Spinasterol	No	-0.664	No	2000	Inactive	Inactive	Active	Inactive
Hexahydrofarnesyl acetone	No	0.244	Yes	5000	Inactive	Inactive	Inactive	Inactive
Lauric acid	No	-0.340	Yes	900	Inactive	Inactive	Inactive	Inactive
Myristic acid	No	-0.559	Yes	900	Inactive	Inactive	Inactive	Inactive
beta-Ionone	No	0.416	Yes	4590	Inactive	Inactive	Inactive	Inactive
Phytol	No	0.050	Yes	5000	Inactive	Inactive	Inactive	Inactive

Note: * = Control ligands; M = Mutagenicity; MTD = Maximum Tolerated Dose; SS = Skin Sensitization; LD50 = Lethal Dose 50; HT = Hepatotoxicity; CG = Carcinogenicity; IT = Immunotoxicity; and CT = Cytotoxicity; Red color indicates values that do not meet the parameters.

Based on the toxicity prediction results, most of the test ligands did not show toxic properties. However, only 10 test ligands were predicted to be non-toxic in all toxicity parameters tested. The test ligands selected for further testing at the molecular docking process are the test ligands that accomplish bioavailability, pharmacokinetics, and toxicity parameters. Based on the prediction results, three test ligands that accomplished all parameters were obtained, including peonidin, kaempferol, and pelargonidin. Therefore, these three compounds have the potential to have good bioavailability, good pharmacokinetic properties, and are not toxic. Thus, they were selected as the test ligands in the molecular docking process to determine their inhibitory potential against the target protein MMP-1.

Validation of molecular docking method

Validation was carried out to determine the binding site of the natural ligand to the target protein and evaluate the change in position or interaction of the ligand to the protein before and after redocking (Krisnayana et al., 2021). Validation is evaluated based on the root-mean-square deviation (RMSD) value, measures the deviation of atomic position between a reference structure and the simulated structure that is optimally superimposed. The smaller the deviations, the more stable the structure conformation. RMSD value depends on the number of rotatable bonds in the molecules. A molecule with more rotatable bonds has a higher RMSD value (Patil et al., 2021). The acceptable RMSD value in the validation process of molecular docking methods is ≤ 2 Å. The smaller the RMSD value, the more similar the two structures. It indicates a valid docking protocol and can be used for the docking process between the test ligand and the target protein (Girsang et al., 2019). The validation results show that the RMSD value of natural ligand (PLH) re-docked on target protein (1HFC) is 1.95 Å. It is considered fairly good and indicates that the docking protocol was valid.

Visualization of the overlay of the redocking ligand with the natural ligand (PLH) as the reference ligand is shown in Figure 4. The redocking ligand shows the same orientation as the reference ligand, apart from a shift in position. The validation results and docking protocols used are presented in Table 4.

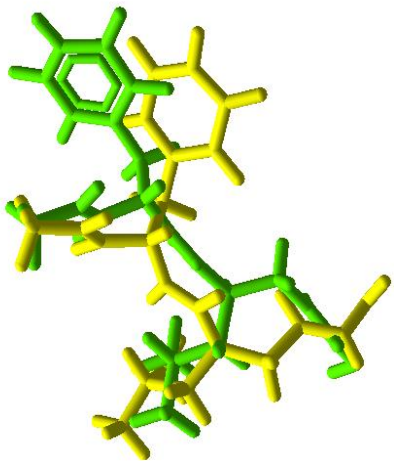

Figure 4. Overlays of Redocking Ligand (Yellow) with Reference Ligand (Green) at Target Protein MMP-1 (PDB ID: 1HFC) with RMSD 1.95 Å.

Table 4. Validation results of molecular docking method

Docking Protocols	Results
Protein	1HFC
Ligand	PLH
Radius	15
Cavity	46.08
Center Coordinate X, Y, Z	25.09; 22.49; 24.03
RMSD	1.95 Å
Hydrogen Bond	Ala182, Glu219, Gly179, His218, His222, Leu181, Pro238, Tyr240
Hydrogen Bond Redocking	Ala182, Asn180, Glu219, Gly179, Leu181, Tyr240

Remarks: Blue color indicates the interaction at the same amino acid residue as reference ligand (PLH) before redocking.

The binding site radius and center coordinates were set, adjusting to the size of the reference ligand used. The redocking results showed that six amino acids interacting with the target protein (MMP-1) similar to the reference ligand through the amino acid residues Ala182, Asn180, Glu219, Gly179, Leu181, Tyr240 located in the area of the target protein binding site (Lee et al., 2020). The interactions were hydrogen bonds that had considerably strong interactions. Thus, the validation results are acceptable, and the redocking protocol can be used in the molecular docking process because the RMSD value is ≤ 2 Å. Furthermore, the redocked ligand shows the same binding interaction with the reference ligand forming hydrogen bonds with the six amino acid residues on the MMP-1 binding site.

Molecular docking

Molecular Docking was performed to predict the potential similarity of the activity of the test ligand with the control ligand in inhibiting the target protein (MMP-1). Molecular docking is evaluated based on the rerank score parameter and the interaction formed. The rerank score indicates the binding energy required to form a bond between the ligand and the target protein. The smaller rerank score means the less energy is needed to bind and the more stable the bond formed between the ligand and target protein so that the ligand has better potential to interact with the target protein (Diningrat et al., 2021).

Based on molecular docking, the results suggest that test ligands have better binding potential than control ligands, with the lowest rerank score owned by peonidin of -108.807 kcal/mol, followed by kaempferol at -99.9796 kcal/mol, and pelargonidin at -98.9128 kcal/mol, as shown in Table 5. The molecular docking results also predicted that the test ligands have similar potential activity with control ligands because they formed the same interaction on the target protein through hydrogen bonds. A ligand could bind to amino acid residues around the target protein binding site by forming interactions such as hydrogen bonds (Diningrat et al., 2021). The hydrogen bond interaction between the ligand and the amino acid residues on the target protein can be seen in Table 6. Kaempferol interacts with the target protein by forming hydrogen bonds at the same amino acid residues as the control ligands, including Ala182, Glu219, and Leu181 at the distance of 2.82-3.36 Å. Pelargonidin and peonidin also form the same hydrogen bonds as the control ligands at residues Ala182, Asn180, and Leu181 at the distance of 2.73-3.14 Å. Residues Ala182, Asn180, Glu219, and Leu181 are known to be residues found in the MMP-1 binding site (Lee et al., 2020). The visualization result of molecular docking shows that the test ligands and control ligands are seen in the same binding cavity on the target protein, as shown in Figure 5. Therefore, the test ligands show the same ability as the control ligands in inhibiting the target protein MMP-1. The bond distance also affected the interaction between the ligand and the target protein. The bonds with closer distance are much stronger and breaking the bond will be more difficult because it takes much energy to break the bond. The average hydrogen bonds distance in ligand and protein complexes is generally in the range of 2.8-3.1 Å (Lee et al., 2020). Thus, the hydrogen bond formed between the test ligand and the target protein MMP-1 is stable and has good bond strength.

Based on in vitro research, flavonoids and anthocyanins contained in pomegranate powder are known to inhibit MMP-1 activity in UVB-induced human primary dermal fibroblast-neonatal (HDF) cells (Lee et al., 2018). Another study was also showed that kaempferol contained in *Punica granatum* (PG) extract is known to act as an anti-photoaging agent by inhibiting MMP-1 expression in UV-irradiated cultured human skin fibroblasts (Folmer et al., 2014). The results of this study support that peonidin, kaempferol, and pelargonidin potentially have activity as anti-photoaging by inhibiting MMP-1.

Table 5. Molecular docking results

Ligand	Rerank score (kcal/mol)	Hydrogen Bond and Distance (Å)
PLH*	-94.2573	Ala182 (3.46), Asn180 (3.41), Glu219 (3.11), Gly179 (2.73), Leu181 (2.75), Tyr240 (2.77)
Doxycycline*	-47.3035	Ala182 (2.21 and 3.14), Asn180 (2.90), Glu219 (2.56), Gly179 (3.10), His218 (3.29), Leu181 (2.80), Pro238 (2.58 and 2.52)
Kaempferol	-99.9796	Ala182 (2.83 and 2.82), Arg214 (2.64), Glu219 (3.31), Leu181 (3.36), Leu235 (3.40), Ser239 (2.86), Tyr237 (2.92)
Pelargonidin	-98.9128	Ala182 (2.84 and 2.73), Arg214 (3.18 and 2.78), Asn180 (3.14), Leu181(2.96), Leu235 (3.43), Ser239 (3.04), Tyr237 (3.07)
Peonidin	-108.807	Ala182 (2.85 and 2.73), Arg214 (3.16 and 2.77), Asn180 (3.14), Leu181 (2.98), Leu235 (3.39), Ser239 (3.07), Tyr237 (3.07)

Remarks: * = Control ligands; Blue color indicates the same amino acid residue as the control ligand.

Table 6. Visualization of molecular docking

Bioactive Compounds	Visualization 3D	Visualization 2D
PLH	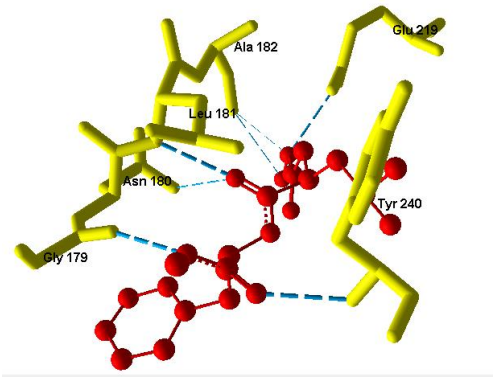	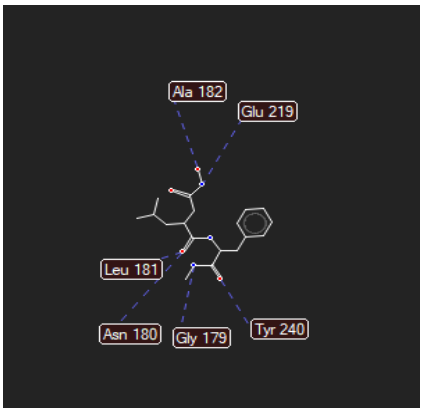
Doxycycline	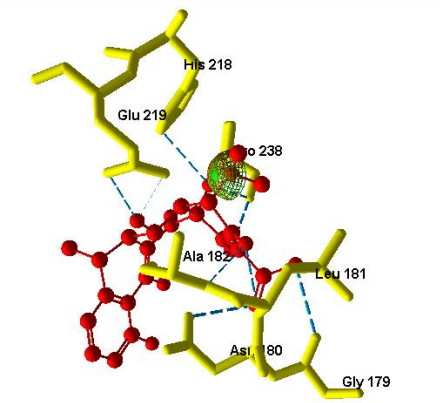	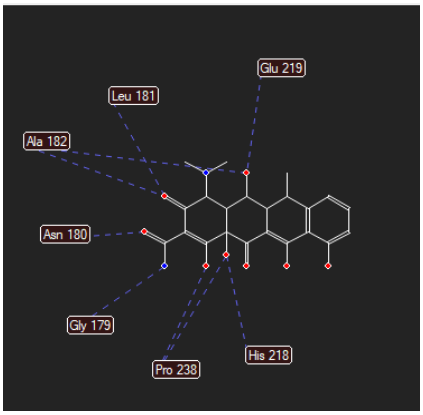
Kaempferol	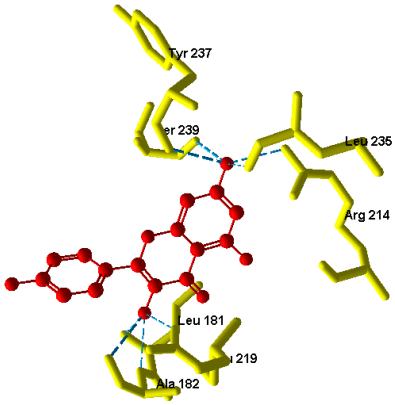	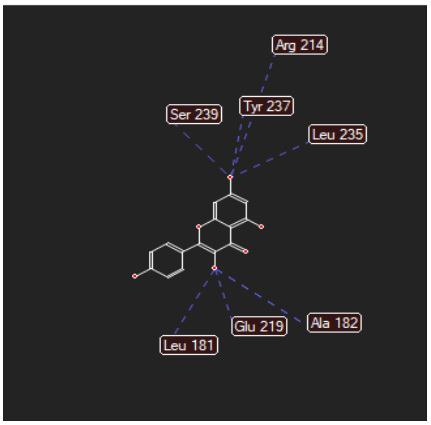

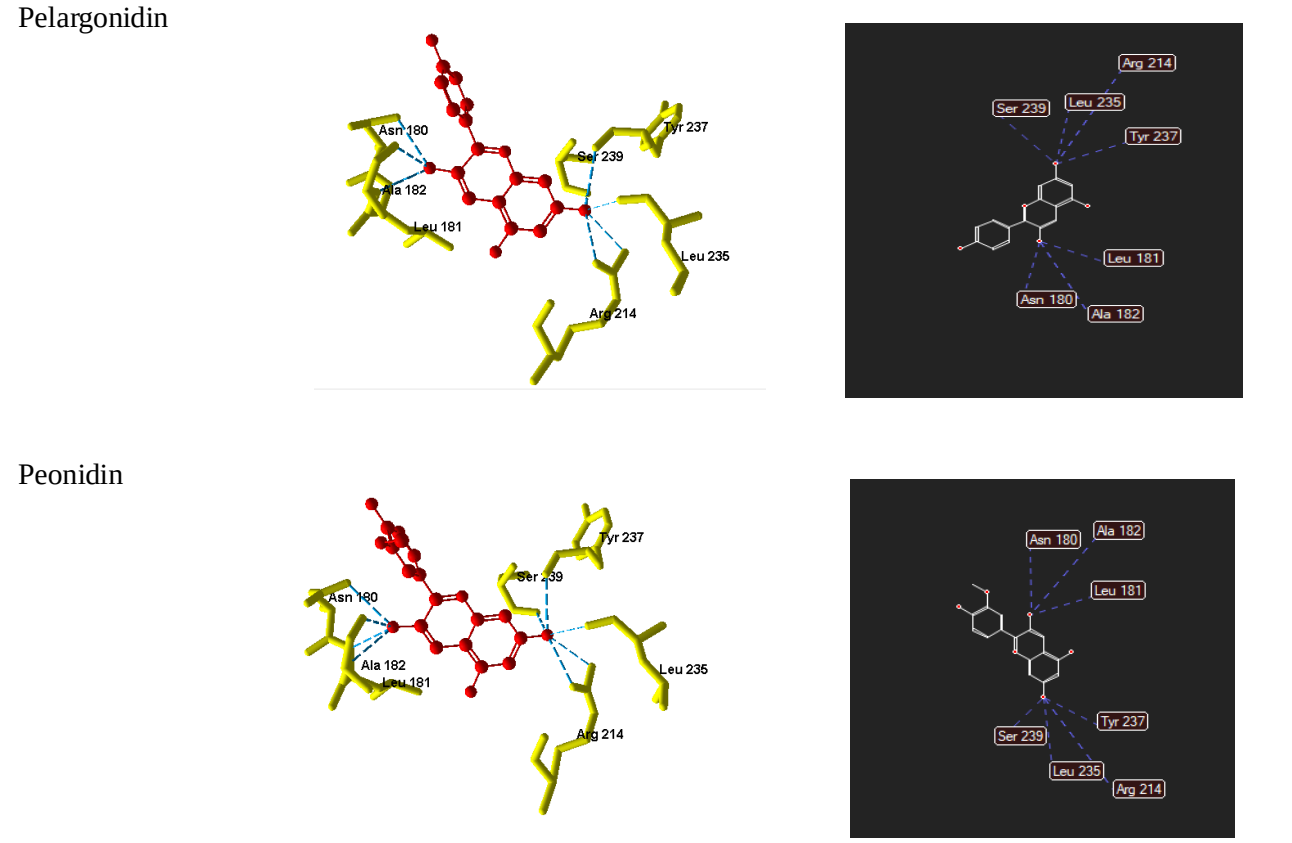

Figure 5. Visualization of molecular docking between ligands and target protein MMP-1 (PDB ID: 1HFC). A = Natural Ligand (PLH); B = Doxycycline; C = Kaempferol; D = Pelargonidin; E = Peonidin; and Red circles indicate the interaction position of the ligands in the binding site of the target protein MMP-1.

Conclusions

Peonidin, kaempferol, and pelargonidin are bioactive compounds of *I. balsamina L.* selected as test ligands in molecular docking prediction. These compounds are predicted to have good bioavailability and pharmacokinetic characteristics and not toxic. Based on molecular docking predictions, peonidin, kaempferol, and pelargonidin are predicted to have good potential in inhibiting MMP-1 as indicated by their lower rerank score and formed the same interaction compared to that of control ligands. Thus, these compounds could be developed as anti-photoaging compound candidates. Further research is needed to validate the prediction results in this study by conducting both in vitro and in vivo studies.

Declarations

Conflict of interests The authors declare no competing interests.

References

Amer, R. I., Ezzat, S. M., Aborehab, N. M., Ragab, M. F., Mohamed, D., Hashad, A., Attia, D., Salama, M. M., and El Bishbishy, M. H. (2021) 'Downregulation of MMP1 expression mediates the anti-aging activity of Citrus sinensis peel extract nanoformulation in UV induced photoaging in mice', *Biomedicine and Pharmacotherapy*, 138, pp. 1-16

Arivazhahan, A. (2019) *Introduction to Basics of Pharmacology and Toxicology: Volume 1: General and Molecular Pharmacology: Principles of Drug Action*. Singapore: Springer Nature Singapore.

Azman, M. Sabri A. H, Anjani Q. K., Mustaffa, M. F., and Hamid K. A. (2022) 'Intestinal absorption study : Challenges and absorption enhancement strategies in improving oral drug delivery', *Pharmaceuticals*, 15(8), pp. 975–998

Banerjee, P., Eckert, A. O., Schrey, A. K., and Preissner, R. (2018) 'ProTox-II: A webserver for the prediction of toxicity of chemicals', *Nucleic Acids Research*, 46, pp. 257–263

Bardal, S. K., Waechter, J. E., and Martin, D. S. (2011) *Applied Pharmacology*. Amsterdam: Elsevier.

Brogi, S. Ramalho, T. C., Kuca, K., Medina-Franco, J. L., and Valko, M. (2020) 'Editorial: In silico methods for drug design and discovery', *Frontiers in Chemistry*, 8, pp. 1-5

Chatterjee, B., Sengupta, P., and Tekade, R. K. (2021) 'Pharmacokinetic Characterization of Drugs and New Product Development' in Tekade, R. K. (eds.) *Biopharmaceutics and Pharmacokinetics Considerations*. Cambridge: Academic Press, pp. 195–277.

Coimbra, J. T. S., Feghali, R., Ribeiro, R. P., Ramos, M. J., and Fernandes, P. A. (2021) 'The importance of intramolecular hydrogen bonds on the translocation of the small drug piracetam through a lipid bilayer', *Royal Society of Chemistry Advances*, 11, pp. 899–908

Diningrat, D. S., Sari, A. N., Harahap, N. S., and Kusdianti (2021) 'In silico study of the toxicity and antiviral activity prediction of jamblang (*Syzygium cumini*) leaves essential oil as ace2 inhibitor', *Pharmacologyonline*, 3, pp. 1334–1351

Feltrin, C., Farias I, V., Sandjo L, P., Reginatto, F. H., and Simoes C. M. O. (2020) 'Effects of standardized medicinal plant extracts on drug metabolism mediated by CYP3A4 and CYP2D6 enzymes', *Chemical Research in Toxicology*, 33(9), pp. 2408–2419

Firdausy, A. F., Muti'ah, R., and Rahmawati, E. K. (2020) 'Predicting pharmacokinetic profiles of sunflower's (*Helianthus annuus L.*) active compounds using in silico approach', *Journal of Islamic Medicine*, 4(1), pp. 1–7

Folmer, F., Basavaraju, U., Jaspars, M., Hold, G., El-Omar, E., Dicato, M., and Diederich, M. (2014) 'Anticancer effects of bioactive berry compounds', *Phytochemistry Reviews*, 13(1), pp. 295–322

Girsang, E., Ginting, C. N., Lister, I. N. E., Widowati, W., Wibowo, S. H. B., Perdana, F. S., and Rizal, R. (2019) 'In silico analysis of phytochemical compound found in snake fruit (*Salacca zalacca*) peel as anti-aging agent', *Thai Journal of Pharmaceutical Sciences*, 43(2), pp. 105–109

Kalepu, S., Manthina, M., and Padavala, V. (2013) 'Oral lipid-based drug delivery systems – an overview', *Acta Pharmaceutica Sinica B*, 3(6), pp. 361–372

Krisnayana, I. G. B., Febyani, P. D., Sari, I. A. Y. P., and Laksmiani, N. P. L. (2021) 'Molecular docking of lutein as anti-photoaging agent in silico', *Pharmacy Reports*, 1(1), pp. 1-6

Lee, D. G., Choi, B. R., Ku, S. K., Kang, S. J., Park, H. R., Sung, M. S., Lee, Y. J., and Park, K. M. (2018) 'In vitro anti-skin-aging effects of dried pomegranate concentrated powder', *Society of Preventive Korean Medicine*, 22(2), pp. 109–123

Lee, K. E., Bharadwaj, S., Yadava, U., and Kang, S. G. (2020) 'Computational and in vitro investigation of (-)- epicatechin and proanthocyanidin b2 as inhibitors of human matrix metalloproteinase 1', *Biomolecules*, 10(10), pp. 1–25

Lipinski, C. A., Lombardo, F., Dominy, B. W., and Feeney, P. J. (2012) 'Experimental and computational approaches to estimate solubility and permeability in drug discovery and development settings', *Advanced Drug Delivery Reviews*, 64, pp. 4–17

Liu, T., Oprea, T., Ursu, O., Hasselgren, C., and Altman R. B. (2016) 'Estimation of maximum recommended therapeutic dose using predicted promiscuity and potency', *Clinical and Translational Science*, 9(6), pp. 311–320

Mcginnity, D. F., and Grime, K. (2017) 'ADME Optimization in Drug Discovery' in *Comprehensive Medicinal Chemistry III*. Third Edit. Amsterdam: Elsevier, pp. 34–44.

Morris-Schaffer, K. and McCoy, M. J. (2021) 'A review of the LD50 and its current role in hazard communication', *ACS Chemical Health and Safety*, 28(1), pp. 25–33

Patil, R., Chikhale R., Khanal, P., Gurav, N., Ayyanar, M., Sinha, S., Prasad, S., Dey, Y. N., Wanjari M., and Gurav, S. S. (2021) 'Computational and network pharmacology analysis of bioflavonoids as possible natural antiviral compounds in COVID-19', *Informatics in Medicine Unlocked*, 22, pp. 1-24

Paul, A. (2019) 'Drug Distribution' in Raj, G. M., and Raveendran, R. (eds) *Introduction to Basics of*

Pharmacology and Toxicology. Singapore: Springer Nature Singapore, pp. 89–98.

Pires, D. E. V., Blundell, T. L., and Ascher, D. B. (2015) 'pkCSM: Predicting small-molecule pharmacokinetic and toxicity properties using graph-based signatures', *Journal of Medicinal Chemistry*, 58(9), pp. 4066–4072

Pittayapruek, P., Meephansan, J., Prapapan, O., Komine, M., and Ohtsuki, M. (2016) 'Role of matrix metalloproteinases in Photoaging and photocarcinogenesis', *International Journal of Molecular Sciences*, 17(6), pp. 1-20

Reilly, D.M. and Lozano, J. (2021) 'Skin collagen through the lifestages: importance for skin health and beauty', *Plastic and Aesthetic Research*, 8, pp. 1-24

Ronsisvalle, S., Panarello, F., Longhitano, G., Siciliano, E. A., Montenegro, L., and Panico, A. (2020) 'Natural flavones and flavonols : Relationships among antioxidant activity , glycation , and metalloproteinase inhibition', *Cosmetics*, 7(3), pp. 71–85

Roy, K., Kar, S., and Das, R. N. (2015) *Understanding the Basics of QSAR for Applications in Pharmaceutical Sciences and Risk Assessment*. Amsterdam: Elsevier Inc.

Ruela, A. L. M., Perissinato, A. G., Lino, M. E. S., Mudrik, P. S., and Pereira, G. R. (2016) 'Evaluation of skin absorption of drugs from topical and transdermal formulations', *Brazilian Journal of Pharmaceutical Sciences*, 52(3), pp. 527–544

Ruswanto, R., Mardianingrum, R., and Yanuar, A. (2022) 'Computational studies of thiourea derivatives as anticancer', *Jurnal Kimia Sains dan Aplikasi*, 25(3), pp. 87–96

Shaker, B., Ahmad, S., Lee, J., Jung, C., and Na, D. (2021) 'In silico methods and tools for drug discovery', *Computers in Biology and Medicine*, 137, pp. 1-15

Sparavigna, A. (2020) 'Role of the extracellular matrix in skin aging and dedicated treatment - State of the art'. *Plastic and Aesthetic Research*, 7(14), pp. 1-6

Utami, N. (2014) 'Suku *Balsaminaceae* di Jawa: Status taksonomi dan konservasinya (The Balsaminaceae family in Java: Taxonomic status and conservation)', *Berita Biologi*, 13(1), pp. 49–55 [In Indonesian]

Yasmeen, S., and Gupta, P. (2019) 'Interaction of selected terpenoids from *Dalbergia sissoo* with catalytic domain of Matrix Metalloproteinase-1: An in silico assessment of their anti-wrinkling potential', *Bioinformatics and Biology Insights*, 13, pp. 1-11

Ye, K., Yang, X., Ji, Y., and Wang, M. (2021) 'A system for determining maximum tolerated dose in clinical trial', *Statistical Theory and Related Fields*, 5(4), pp. 288–302